

# The Main Lighting Direction Estimation for the Uniform Texture Images

Yujuan Sun\*, Qingtang Su\*, Xiaofeng Zhang\*, and Peng Liu\*

\* Ludong University, Yantai, China

E-mail: syj\_anne@163.com Tel/Fax: +86-15853578596

**Abstract**—In this paper, a method for lighting directions estimation of the uniform texture images has been proposed. The proposed algorithm does not require training database, and only utilizes one input image for estimating the lighting directions. By detecting the largest direction of the brightness changes of the input image, the azimuth angle of the light source can be estimated. The slant angle is estimated by generating a random texture, whose density parameter and lighting directions are controllable. By comparing the intensity distribution between the input image and the generated texture, the slant angle can also be estimated.

## I. INTRODUCTION

In theory, it is possible to estimate the lighting direction only from one single input image, because that the lighting conditions can be observed as a part of the albedo for the image. Actually, if the object's surface is uneven, it will exist different kinds of shadow (such as the self shadow and cast shadow) along the direction of the light propagation. Since the direction of light propagation is straight, and the light direction and the shadow is always orthogonal to each other. Therefore, the brightness change is significant along the direction of light propagation. By detecting the largest direction of the brightness change for the input image, the azimuth angle of the light source can be estimated. In addition, a random texture has been generated to assist in estimating the slant angle of the input texture image.

## II. RELATED WORK

Robust estimation of lighting directions is important in some computer-vision applications, such as rendering the real-world scene and 3D reconstruction based on photometric stereo [?]. The first kind of estimation algorithms for lighting direction needed to know the geometry of the object. In [?], a simple method for estimation of point light-sources was proposed. The parameters of a light source at finite distance can be estimated by shading on an object with known geometry and Lambertian reflectance. Tachikawa et al. [?] proposed a method to determine the lighting direction and diffuse reflectance property from two images under different light conditions. In [?], an approach for light source position and reflectance estimation from a single view was proposed, but need to know the surface normals of the object in the image, which limits the real application.

The second kind of estimation algorithms required the special feature for the input image, or under the special light conditions. Li et al. [?] presented a method that integrated

multiple cues from shading, shadow and specular reflectance for estimating directional illumination in a textured scene. This method was suitable for the texture with obvious cast shadow. In [?], an algorithm for estimating the projected light source direction from a single image was proposed. The requirement of this method was that there existed a segmentation of an occluding contour of an object with locally Lambertian surface reflectance in the image. The method in [?] can separate the shading effects of a static outdoor scene due to the sunlight and skylight. Hougen and Ahuja [?] estimated the light source distribution based on the assumption of a lighting model with point lights at infinity, which also limited the related application in complex lighting conditions.

The third kind of estimation algorithm had to used the special active light source or specialized acquisition device to capture the input image. An effective way to recover the illumination by using structure light is proposed in [?]. The last kind of estimation algorithms for lighting direction were applied for the texture image. [?], [?] developed a theory for recovering the illuminants azimuthal angle from a single image under a Lambertian model, but the estimation for slant angle was not given in these paper. Ikeuchi and Sato [?] proposed a method to estimate the parameters of reflection model and direction of the light source from a pair of range and intensity image. This method assumed that the reflectance was uniform over the whole object. Literatures [?], [?], [?] estimated the lighting direction based on the training method, and the azimuth angle of the lighting direction can be accurately estimated at the same time for texture classification. But these methods required a lot of training samples and the time complexity was high for lighting parameter estimation, which is the limitation of previous algorithms for real application.

## III. THE PROPOSED METHOD

We proposed an estimation method for lighting directions of the uniform texture images. In this algorithm, the lighting direction can be real-time estimated just from a single input image. To simplify the discussion, we assume the following constraints, and the issue of estimation for lighting directions will be alleviated in the experiments.

(1) Reflection characteristics satisfies Lambertian model. The light source is single and uniform parallel, however, the light intensity and direction (the slant and azimuth angles) are unknown.

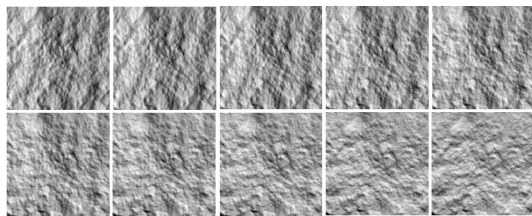


Fig. 1. The rock texture images captured in different azimuth angle (from left to right, from top to bottom, the azimuth is 0°, 10°, ..., 90° respectively).

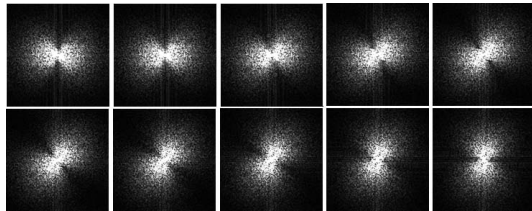


Fig. 2. The frequency domain of the images in Fig.1 (from left to right, from top to bottom, the azimuth is 0°, 10°, ..., 90° respectively).

(2) The albedo of the object surface is uniform, namely the albedo of the object should not have obvious texture direction.

Therefore, for estimation of lighting directions, our task is how to effectively and accurately detect the main direction. That is to say, the slant and azimuth angles need to be estimated.

Fig.1 shows the rock texture images captured in different azimuth angle. From left to right, from top to bottom, the azimuth is 0°, 10°, 20°, ,90° respectively. For the texture images in Fig.1, we can see that the human eyes may not be able to accurately judge the azimuth angle of the light source. However, when the images in Fig.1 are transformed from spatial domain into frequency domain, the azimuth change of the light source can be clearly observed. Fig.2 shows the frequency domain of the images in Fig.1. From Fig.2, it can be seen that the frequency spectrums are gradually rotating from 0 degree to 90 degree.

#### A. Estimating the azimuth angle of the input texture image

Inspired by the perception model of human eye [?], we use the visual cortex enhancement model to detect the main direction (azimuth angle) in frequency domain for the input texture image. Physiological researches show that the human visual system has the characteristics of rapid perception outline, and the Gabor function can well simulate these physiological characteristics of human eye perception. The 2-D Gabor function is defined as follows:

$$Gabor(u, v, \sigma) = \frac{1}{2\pi\sigma^2} e^{-\frac{u^2+v^2}{\sigma^2}} \quad (1)$$

where  $\sigma$  is the variance of Gabor function,  $(u, v)$  represents the direction of Gabor function and is obtained by rotating the  $(x, y)$  in Cartesian coordinate system.  $(u, v)$  can be expressed

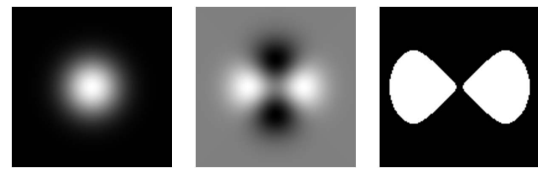


Fig. 3. Human eye perception model based on Gabor function (from left to right: 2D Gabor function, edge enhancement model, direction detection template).

by

$$\begin{bmatrix} u \\ v \end{bmatrix} = \begin{bmatrix} \cos \theta & \sin \theta \\ -\sin \theta & \cos \theta \end{bmatrix} \begin{bmatrix} x \\ y \end{bmatrix} \quad (2)$$

where  $(x, y)$  represents the center of human eye receptive field;  $\theta$  represents the rotation angle, namely the orientation of the human receptive field. Then  $Gabor(u, v, \sigma)$  can also be represented by  $Gabor(x, y, \sigma, \theta)$ .

The human eye also has the function of edge enhancement. If an edge is a continuous contour, there will be an enhanced effect along the edge in human eyes. Equation (3) has been used to represent the edge enhancement function of human eyes.

$$E(x, y, \sigma, \theta) = Gabor(x, y, \sigma, \theta) \times (x^2 - y^2) \quad (3)$$

In order to estimate the main direction of the frequency domain, a threshold  $thr$  can be set to design the direction detection templates  $T(x, y, \sigma, \theta)$  for the texture edge enhancement model as in equation (4).

$$T(x, y, \sigma, \theta) = \begin{cases} 1 & E(x, y, \sigma, \theta) \geq thr \\ 0 & E(x, y, \sigma, \theta) < thr \end{cases} \quad (4)$$

where the value of  $thr$  is set according covering 50% energy of  $E$ .

Fig.3 shows the 2D Gabor function, edge enhancement model and direction detection template. By computing the statistical averages of the product between frequency domain and the direction templates, and recording the angle of maximum according to equation (5), we can estimate the azimuth angle of the input texture image as follows:

$$A_z = \{\theta \mid \max_{\theta} \{\text{mean}(F(I) * T(x, y, \sigma, \theta))\}\}, \quad \theta = 0^\circ, 5^\circ, \dots, 180^\circ \quad (5)$$

where  $A_z$  is the estimated azimuth angle,  $F(I)$  is the frequency domain of the input image.  $*$  represents the convolution of  $F$  and  $T$ .

#### B. Estimating the slant angle of the input texture image

Fig.4 shows the intensity images under different slant angles and same azimuth angle (azimuth=0°) of the rock texture. We can see the intensity of the image at 0° slant angle is uniform and have no obvious shadow. With the gradual increase of slant angle, the structure of the texture image will not change, but the intensity contrast (mainly caused by shadow) will appear huge changes. Hence we can observe that the slant angle is related with the distribution of shadow. Therefore the intensity

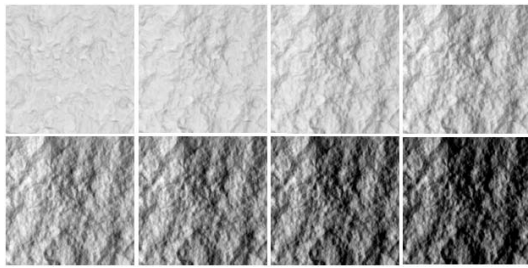


Fig. 4. Intensity images under different slant angle (From left to right, from top to bottom, the slant angle is  $0^\circ, 10^\circ, \dots, 70^\circ$  respectively).

distribution, such as image histogram, can be used to estimate the slant angle of the input texture image.

In order to accurately estimate the slant angle of an input texture image, we generate a random height map controlled by density parameter  $\sigma$ . The density parameter can control the change rate of the height map. If  $\sigma$  is small, the change of height map is dramatic. If  $\sigma$  is big, the change of height map is gentle.

By changing  $\sigma$  and slant angle of the light source, we can obtain several generated images, which have different slant angle with the input image. By searching the most similar generated image with the input image, the slant angle can be estimated. The slant angle estimation algorithm is described as follows:

Initialization: initial density parameters ( $\sigma$ ) of the random height map; Input: a texture image  $I$

(1) Generate the height map ( $TI$ ) controlled by  $\sigma$  and estimate the slant angle of  $I$  by using equation (6).

$$slant = \{\theta, |similar_{max}(I, TI(\theta)), \theta = 0^\circ, 5^\circ, 10^\circ, \dots, 70^\circ\} \quad (6)$$

where  $similar(I, TI(\theta))$  is the similarity measure function by computing the maximum similarity of  $I$  and  $TI$  in different slant angles to estimate the slant angle of input texture image. Because of the slant angle greater than 70 degrees will cause obvious cast shadows, so we only consider of within 0 to 70 degrees in this paper. The function of  $similar(I, TI(\theta))$  is defined as follows:

$$similar(\theta) = \lambda_1 S_1(I, TI(\theta)) + \lambda_2 S_2(I, TI(\theta)) \quad (7)$$

where  $S_1(I, TI(\theta))$  represents the local similarity (the gray value of image block is used in our algorithm) between  $I$  and  $TI$ ;  $S_2(I, TI(\theta))$  represents the global similarity (image histogram is used in our algorithm) between  $I$  and  $TI$ ;  $\lambda_1$  and  $\lambda_2$  represents the weight of  $S_1$  and  $S_2$  respectively.

(2) By using the estimated slant of (1) to get  $TI(slant)$ , we can change parameter  $\sigma$  to generate  $TI(slant, \sigma)$ . Where  $\sigma$  is changed in two direction of positive and negative ( $\sigma_{new} = \sigma \pm 0.1n$ ),  $n = 1, 2, \dots, N$ ,  $N$  represents the maximum range of  $\sigma$ . When the function of similarity in equation (8) obtains the maximum value, we can obtain the local optimal value of  $\sigma$ .

$$similar_{max}(\delta) = \lambda_1 S_1(I, TI(slant, \delta)) + \lambda_2 S_2(I, TI(slant, \delta)) \quad (8)$$

(3) If similarity function no longer changes or the maximum number of iteration is reached, then stop; Otherwise, go to (1).  
Output: the slant angle:  $\theta$ ; the density parameter:  $\sigma$ .

#### IV. EXPERIMENTS AND ANALYSIS

In order to verify the effectiveness of the proposed scheme, the lighting directions (the azimuth and slant angle) for 24 different kinds of texture images in Photex Database are used to evaluate the performance of our proposed framework. The azimuth angle includes 0, 30, 50, 60, 80, 90, 110, 120, 140, 150 and the slant angle is 30, 45, 60 degree. In total, there are 142 texture images with different lighting directions, which include some surface consistency textures and inconsistency textures, have been tested and estimated in our experiments.

##### A. Estimating the azimuth angle of an input texture image

We firstly classify the 24 kinds of texture images to five classes, denoted by A, B, C, D and E. We select one typical image from each class to show the estimated results. The image in first column of Table 1 is the texture of 0 azimuth degree and with the same slant angle, and the words under the image describe its category and name. The second column in Table 1 is the ground truth (G.T.) azimuth angle of the input image. The third column in Table 1 is the estimated azimuth using our method. The last column shows the estimated error between G.T. azimuth and Estimated azimuth. From the last column we can see that the estimated results of class A, C and E is more accurate than that of class B and D.

Since this paper focus on considering the uniform texture image, the estimated error is big for class B and D. It is mainly because the texture images of class B and D have obvious texture direction. The texture direction seriously affects the estimation of azimuth angle, which is our future work.

##### B. Estimating the slant angle of an input texture image

For further verifying the effectiveness of our algorithm for slant angle estimation, the 24 kinds of texture images in Photex database had been tested. Table 2 shows the estimated results for 24 kinds of texture images. The words in first column, for example "aab45-0" represent the image "aab" at slant angle of 45 degree and azimuth angle of 0 degree. As shown in Table 2, our algorithm can produce promising and satisfactory results.

From Table 2, we can find that the error of the proposed slant angle estimation algorithm is small for different kinds of texture image, excluding three kind of texture "ach", "aci" and "acj". The main reason is that the surface texture of "ach", "aci" and "acj" is almost completely black, and most of the reflected light is absorbed in the surface of the black region.

TABLE I  
THE ESTIMATED AZIMUTH ANGLE FOR FIVE TYPICAL KINDS OF TEXTURE IMAGES

Num	G.T.azimuth	Estimated azimuth	Azimuth error
A: aab	0°	0°	0°
	50°	45°	5°
	90°	85°	5°
	110°	105°	5°
	140°	145°	5°
	170°	170°	0°
B: aba	0°	20°	20°
	30°	15°	15°
	60°	25°	35°
	90°	55°	35°
	150°	170°	20°
C: acd	0°	5°	5°
	30°	25°	5°
	60°	55°	5°
	90°	85°	5°
	120°	120°	0°
D: acf	0°	0°	0°
	30°	10°	20°
	90°	90°	0°
	120°	105°	15°
	150°	170°	20°
E: ach	0°	0°	0°
	30°	25°	5°
	60°	55°	5°
	90°	90°	0°
	120°	120°	0°
	150°	155°	5°

V. CONCLUSION

In this paper, we have presented a simple method for estimation of lighting directions for the uniform texture images. The proposed algorithm can estimate the light parameters for the parallel light in the vertical viewing angle. Through estimating the lighting direction of the texture image in Photex database, experimental results show that our method is effective for estimating azimuth angle and slant angle of the uniform texture images.

ACKNOWLEDGMENT

This work was supported by Natural Science Foundation of Shandong (ZR2015FQ011; ZR2014FQ023); National Natural Science Foundation Of China (NSFC) (61271405, 61401413);

TABLE II  
THE ESTIMATED SLANT ANGLE FOR 24 KINDS OF TEXTURE IMAGES

Num	Estimated slant	Error	$\sigma$
aab45-0	50°	5°	0.4
aaf45-0	50°	5°	0.7
aai45-0	45°	0°	0.7
aaaj45-0	50°	5°	0.3
aam45-0	55°	10°	0.4
aan45-0	50°	5°	0.5
aao45-0	55°	10°	0.8
aap45-0	55°	10°	0.6
aar45-0	50°	5°	0.9
aas45-0	45°	0°	1.0
aba45-0	45°	0°	1.0
abj45-0	55°	5°	1.1
abk45-60	50°	10°	0.8
acc45-0	55°	5°	0.6
acd60-0	60°	0°	1.1
ace45-0	60°	15°	1.0
acf60-0	55°	5°	0.9
acg60-0	55°	5°	1.0
ach60-0	70°	10°	1.2
aci30-0	65°	35°	0.2
acj45-0	70°	25°	0.7
ack60-0	60°	0°	0.1
ada45-0	55°	5°	0.6
adb45-0	60°	15°	0.7